Quark cluster probabilities in nuclei

M. Sato* and S. A. Coon
Department of Physics, University of Arizona, Tucson, Arizona 85721

H. J. Pirner
CERN, Geneva, Switzerland

J. P. Vary
Iowa State University, Ames, Iowa 50011
(Received 28 October 1985)

We present results for quark cluster probabilities in nuclei based on the assumptions of the quark cluster model. We first perform numerical evaluations in $a=2$, 3, and 4 nuclei based on realistic nuclear wave functions for the probability that a quark chosen at random in the nucleus is found in a color singlet cluster consisting of 3, 6, 9, etc., quarks. Clustering itself is determined by a geometrical overlap of three-quark systems that depends on a critical distance of separation $2R_c$. A systematic comparison of cluster probabilities obtained for these light nuclei establishes certain features of these results, which are independent of A and of the wave function used. These results are then used to make predictions of quark cluster probabilities in heavier nuclei. We present relationships between our definition of quark cluster probabilities and that of some other efforts.

I. INTRODUCTION AND MOTIVATION

To apply the quark cluster model[1] to experiment, both quark cluster probabilities and the response of the cluster to the experimental probe must be specified. In the case of lepton scattering, the coupling of the photon to the quark is specified by quantum electrodynamics (QED), but the response of the nucleus must be developed through a model. The quark cluster model[1,2] assumes the scattered quark originates from a color singlet cluster composed of 3, 6, 9, etc., valence quarks. Clusters are defined by the "overlap" of three-quark ($3q$) subsystems, each of which has an assigned critical radius, R_c. Overlap is assumed to occur when two subsystems are separated by a distance $\leq 2R_c$. The position of each $3q$ subsystem is separated by a distance $\leq 2R_c$. The position of each $3q$ subsystem is determined by the nuclear wave function with pointlike nucleons. Then if $R_c=0$, no quark clusters larger than nucleons are formed, and the standard model of the nucleus survives. If R_c is large, say ~ 1.2–1.5 fm, then percolation occurs, and the nucleus has a high probability of being found in a $3A$ quark cluster configuration. In fits to deep inelastic lepton scattering data, we have determined that $R_c=0.50\pm 0.05$ fm, provides a reasonable description to the data on ^{3}He (Refs. 1 and 3) and a satisfactory description of the European Meson Collaboration (EMC) effect.[4] Carlson and Havens[5] used the same model with somewhat higher quark cluster probabilities to fit the EMC effect data. Furthermore, the long-standing mystery of the elastic charge form factor of ^{3}He can be explained with this model.[6]

Here we address the general question of how to use the available information from realistic microscopic nuclear theory to predict the quark cluster probabilities, a necessary ingredient to the quark cluster model. We also attempt to clarify the differences with other definitions of "quark cluster probabilities" that have been proposed.

In recent years, substantial progress has been made in the description of three- and four-body nuclear systems with realistic nucleon-nucleon (N-N) interactions. Wave-function solutions of the few-body Schrödinger equation are available for the Reid soft core (RSC), Hamada-Johnston (HJ), Tamagaki (OPEG-Gaussian soft core with one-pion-exchange tail), and Paris (P) potentials.[7–10] All these potentials were fit to the phase shifts and deuteron properties of the time and, consequently, contain a tensor force, which couples S and D parts of the N-N wave function. Wave functions from the pure S wave Malfliet-Tjon potentials[11] are useful in order to assess the importance of D-state components on quark cluster probabilities. We employ these wave functions here with two major goals:

(1) To evaluate quark cluster probabilities for these light nuclei in the region around $R_c=0.50$ fm and to check the sensitivity to the choice of the N-N interaction.

(2) To examine the results on an appropriate dimensionless scale to look for certain universal features that could be used to extrapolate to heavier nuclei.

Our chief findings are that there is some sensitivity to the choice of the N-N interaction. However, the results for a given nuclear system are highly correlated with the root-mean-square (rms) radius r_m obtained from the same wave function. Thus, a dimensionless scale proportional to R_c divided by the rms radius is introduced, and this rescaling eliminates most of the sensitivity to the interaction. Cross comparisons of results from different A show that quark cluster probabilities are approximately independent of A when plotted vs $R_c/(r_m/A^{1/3})$. This provides results that are useful for extrapolating to heavier nuclei.

II. QUARK CLUSTER PROBABILITIES ($A=2$)

We utilize the full many-body wave function ψ_A for A nucleons, which is specified in coordinate space as a function of internal coordinates only. From ψ_A, we evaluate the full many-body density matrix

$$\rho_A=\psi_A^*\psi_A \ . \tag{1}$$

In what follows, we sum over spin and isospin so that the quark cluster probabilities are spin and isospin average clusters for each nucleus.

For the simplest case of the deuteron, the $i=$three- and six-quark cluster probabilities $\tilde{p}_i^{(A)}$ are given by

$$\tilde{p}_3^{(2)}=\int d^3\mathbf{r}\rho_2(\mathbf{r})\theta_c(r) \ , \tag{2a}$$

$$\tilde{p}_6^{(2)}=\int d^3\mathbf{r}\rho_2(\mathbf{r})[1-\theta_c(r)] \ , \tag{2b}$$

respectively, where $\theta_c(z)\equiv\theta(z-2R_c)=1$ when $|\mathbf{z}|>2R_c$ and is zero otherwise. It is clear that the condition

$$\sum_i \tilde{p}_i^{(A)}=1 \tag{3}$$

is obeyed. Furthermore, on the one hand, the limit in which R_c tends to zero yields $\tilde{p}_3^{(2)}=1$ and $\tilde{p}_6^{(2)}=0$, which we may think of as the limit of conventional nuclear physics, since larger quark clusters do not occur. Then, on the other hand, as R_c gets large, the percolation limit, $\tilde{p}_6^{(2)}=1$ and $\tilde{p}_3^{(2)}=0$, is eventually reached. This sum rule and limiting cases characterize quark cluster probabilities in any nucleus. Here, our primary interest is focused on the region near $R_c=0.50$ fm.

In Fig. 1 we display $\tilde{p}_3^{(2)}$ and $\tilde{p}_6^{(2)}$ as functions of R_c for the RSC, HJ, and P wave functions. The $\tilde{p}_i$ curves are very similar, in spite of the fact that HJ is a "hard core" potential while Reid is a "soft core" potential. We note that differences are especially small in the region around $R_c=0.5$ fm. The precise values for these probabilities at $R_c=0.50$ fm are $\tilde{p}_3^{(2)}=(0.953,0.952,0.950)$ and $\tilde{p}_6^{(2)}=(0.047,0.048,0.050)$ for the (RSC, HJ, P) wave functions, respectively.

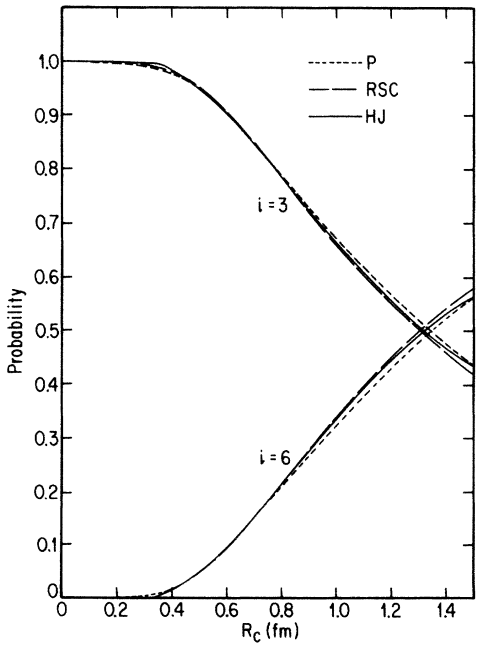

FIG. 1. i-quark cluster probabilities $\tilde{p}_i^{(2)}$ from three model wave functions for ^{2}H as a function of R_c. The potentials are Reid soft core (RSC), Hamada-Johnston (HJ), and Paris (P).

III. QUARK CLUSTER PROBABILITIES ($A=3$)

To treat systems with $A>2$, we will present a specific choice of the coordinate system and conventions. We choose a quark at random from the nucleus and arbitrarily place the label "1" on the $3q$ subsystem from which that quark originated. Then we examine the correlations with all the other subsystems to see where the important overlaps exist to form clusters with the $3q$ subsystem "1." The character of that cluster is defined by the total number of overlapping $3q$ subsystems (allowing for "linear-chain" configurations). Thus, referring to Fig. 2, where we have redundant coordinate vectors for simplicity, we define the respective quark cluster probabilities $\tilde{p}_i^{(3)}$ for the $A=3$ nucleus:

$$\tilde{p}_3^{(3)}=\int d^3x'd^3x''\rho_3(\mathbf{x}',\mathbf{x}'')\theta_c(x')\theta_c(x'') \ , \tag{4a}$$

$$\tilde{p}_6^{(3)}=\int d^3x'd^3x''\rho_3(\mathbf{x}',\mathbf{x}'')\theta_c(x)\times[\theta_c(x')\bar{\theta}_c(x'')+\theta_c(x'')\bar{\theta}_c(x')] \ , \tag{4b}$$

$$\tilde{p}_9^{(3)}=\int d^3x'd^3x''\rho_3(\mathbf{x}',\mathbf{x}'')\times[\bar{\theta}_c(x')\bar{\theta}_c(x'')+\bar{\theta}_c(x')\bar{\theta}_c(x)+\bar{\theta}'_c(x'')\bar{\theta}_c(x)-2\bar{\theta}_c(x)\bar{\theta}_c(x')\bar{\theta}_c(x'')] \ , \tag{4c}$$

where, for simplicity, we use the abbreviation $\bar{\theta}_c(z)\equiv 1-\theta_c(z)$. It is straightforward to verify directly that the sum of Eqs. (4) is unity according to the condition (3).

It should be clear that the complexity of the equations and the calculational effort increases rapidly with A. We also emphasize again that Eqs. (4) illustrate the importance of having the full many-body wave function. The generalization to the A-body problem amounts to a calculation of the expectation value of an A-body operator for each of the $\tilde{p}_i^{(A)}$. We must employ the distribution function, which specifies how all A particles behave simultaneously. Other efforts in the literature have invoked only two-particle correlations and two-body operators and

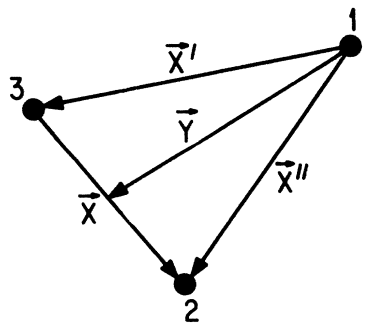

FIG. 2. Coordinate vectors of three-quark subsystems used in Eqs. (4) to define quark cluster probabilities in $A=3$ nuclei.

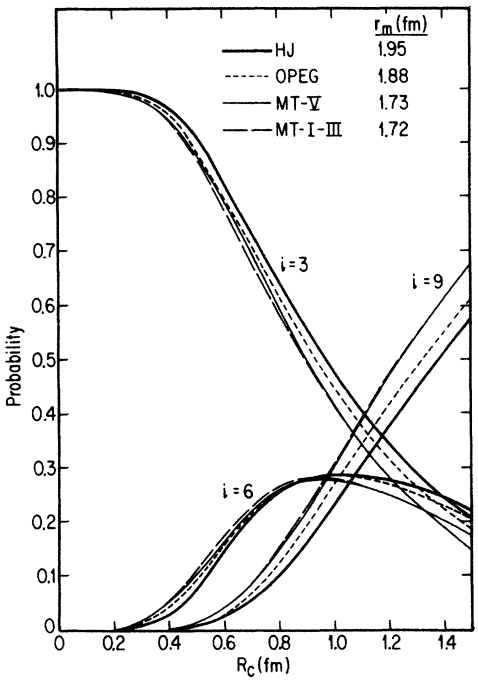

FIG. 3. i-quark cluster probabilities $\tilde{p}_i^{(3)}$ from four model wave functions of the $A=3$ isodoublet. The potentials are HJ, Tamagaki (OPEG), and two S-wave potentials of Malfliet and Tjon (MT V and MT I-III). The isoscalar baryon mass radius $r_m=\langle r^2\rangle^{1/2}$ of each model wave function is also shown. The experimental value of r_m is 1.70±0.02 fm.

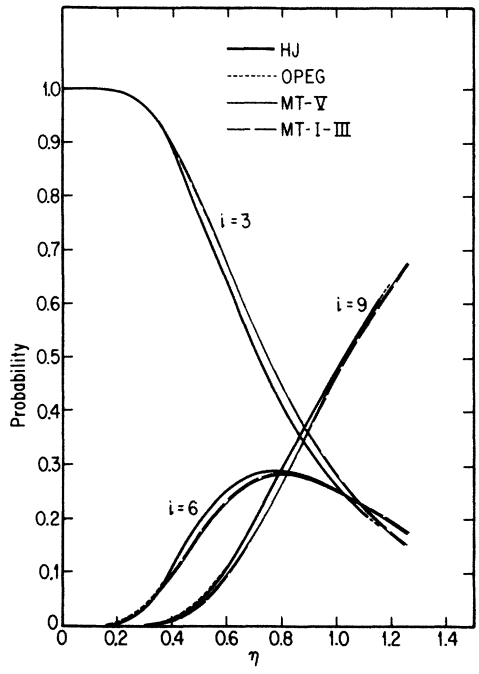

FIG. 4. i-quark cluster probabilities $\tilde{p}_i^{(3)}$ of Fig. 3 plotted as a function of $\eta=R_c/(r_m/A^{1/3})$. The MT potentials nearly coincide, and the HJ and OPEG have nearly the same $\tilde{p}_i^{(3)}$ as a function of η.

are inadequate for our work.[12,13]

In Fig. 3 we present the quark cluster probabilities corresponding to Eqs. (4) as a function of R_c for a variety of realistic and semirealistic nucleon-nucleon potentials.[14,15] In general, they yield quite similar results. Note that the semirealistic Malfliet-Tjon potentials have weaker short-range correlations and tend to have six- and nine-quark cluster probabilities that increase faster with R_c. However, we remark that there is also a correlation between the $\tilde{p}_i$ values and the rms radius of each wave function. Since the $A=3$ nucleus is an isodoublet, we take the rms radius to be the isoscalar (or mass) part. The isoscalar $r_m=\langle r^2\rangle^{1/2}$ is determined by sums of squares of wave function components and is obtained from experimental data as the weighted average of two parts charge radius of ^{3}He and one part charge radius of ^{3}H after a correction for the finite electromagnetic size of nucleons.

Although these results for different interactions are in reasonable agreement with each other, we examine an earlier suggestion[2] that cluster probabilities should be primarily sensitive to the average separation between nucleons in a nucleus, which is related to the rms radius divided by $A^{1/3}$. Thus, we replot the results of Fig. 3 as a function of the dimensionless parameter $\eta\equiv R_c/(r_m/A^{1/3})$, as shown in Fig. 4. As suggested, this brings all the results to even closer agreement. It is important to note that the results of Fig. 3 do *not* scale with the rms radius of ^{3}H nor with ^{3}He, but only with the isoscalar rms radius defined above. Thus, when viewed on this dimensionless η scale, the cluster probabilities are remarkably independent of the N-N interaction. This independence is especially noteworthy when we recall that the realistic interactions include tensor forces, whereas the semirealistic do not. This universality also implies that with the experimental rms of the $A=3$ nucleus we could extract a "corrected" prediction of quark cluster probabilities using the interaction independent results of Fig. 4. The experimental scalar rms radius for pointlike nucleons is 1.70±0.02 fm; it lies at the expected value corresponding to the binding energy of the $A=3$ nucleus.[16]

After presenting the results for $A=4$ and examining the same issues of scaling with average baryon density, we will then compare results between different systems to examine the A dependence of this scaling behavior.

IV. QUARK CLUSTER PROBABILITIES ($A=4$)

The conventions we will use for interparticle vectors are specified in Fig. 5. Again, the use of redundant vectors allows for a simplified presentation of the expressions for the quark cluster probabilities. They are

$$\tilde{p}_3^{(4)}=\int d^3\mathbf{x}'d^3\mathbf{x}''d^3\mathbf{y}'\rho_4(\mathbf{x}',\mathbf{x}''\mathbf{y}')\theta_c(x')\theta_c(x'')\theta_c(y')\ , \tag{5a}$$

$$\tilde{p}_6^{(4)}=\int d^3\mathbf{x}'d^3\mathbf{x}''d^3\mathbf{y}'\rho_4(\mathbf{x}',\mathbf{x}'',\mathbf{y}')[\bar{\theta}_c(x')\theta_c(x'')\theta_c(y')\theta_c(x)\theta_c(y)$$
$$+\bar{\theta}_c(x'')\theta_c(x')\theta_c(y')\theta_c(x)\theta_c(y'')+\bar{\theta}_c(y')\theta_c(x')\theta_c(x'')\theta_c(y)\theta_c(y'')]\ , \tag{5b}$$

$$\tilde{p}_9^{(4)}=\int d^3\mathbf{x}'d^3\mathbf{x}''d^3\mathbf{y}'\rho_4(\mathbf{x}',\mathbf{x}'',\mathbf{y}')$$
$$\times\{\theta_c(x')\theta_c(x)\theta_c(y)[\bar{\theta}_c(x'')\bar{\theta}_c(y')+\bar{\theta}_c(y')\bar{\theta}_c(y'')+\bar{\theta}_c(x'')\bar{\theta}_c(y'')-2\bar{\theta}_c(x'')\bar{\theta}_c(y')\bar{\theta}_c(y'')]$$
$$+\theta_c(y')\theta_c(y'')\theta_c(y)[\bar{\theta}_c(x'')\bar{\theta}_c(x')+\bar{\theta}_c(x'')\bar{\theta}_c(x)+\bar{\theta}_c(x')\bar{\theta}_c(x)-2\bar{\theta}_c(x'')\bar{\theta}_c(x')\bar{\theta}_c(x)]$$
$$+\theta_c(x'')\theta_c(x)\theta_c(y'')[\bar{\theta}_c(x')\bar{\theta}_c(y')+\bar{\theta}_c(x')\bar{\theta}_c(y)+\bar{\theta}_c(y')\bar{\theta}_c(y)-2\bar{\theta}_c(x')\bar{\theta}_c(y')\bar{\theta}_c(y)]\}\ . \tag{5c}$$

We have developed the full expression for $\tilde{p}_{12}^{(4)}$, but it is far too lengthy to warrant its detailed presentation. In the computer code condition (3) was satisfied with Eqs. (5) plus our expression for $\tilde{p}_{12}^{(4)}$. Condition (3) thus provides a numerical consistency check on the derivation and the code. However, it is simpler to evaluate $\tilde{p}_{12}^{(4)}$ through the use of Eqs. (3) and (5). That is,

$$\tilde{p}_{12}^{(4)}=1-\tilde{p}_3^{(4)}-\tilde{p}_6^{(4)}-\tilde{p}_9^{(4)}\ . \tag{5d}$$

The wave functions we use for $A=4$ are those of the Hokkaido group[17,18] for the RSC, P, and HJ potentials. They construct a variational wave function in the form $\psi=F\phi$ on the basis of multiple scattering theory, where ϕ is a simple initial wave function. The multiple scattering operator F is replaced by two-body correlation functions obtained from the two-body Brueckner reaction matrix. The wave function is then improved variationally. A recent discussion of this method (the ATMS method) and the quasi-random number (QRN) method for evaluation of the multidimensional integrals of Eqs. (5) is presented in Ref. 19.

We present results for $\tilde{p}_i^{(4)}$ in Figs. 6(a) and (b) as a function of R_c for these N-N potentials. The results are nearly independent of the choice of N-N potential over the entire range of R_c. As in the $A=3$ case, the small differences that occur appear to be well correlated with the rms radius of the wave function. We verify this by replotting the $\tilde{p}_i^{(4)}$ results as a function of η in Figs. 7(a) and (b). Now, the differences are so small as to be barely visible in the graphs.

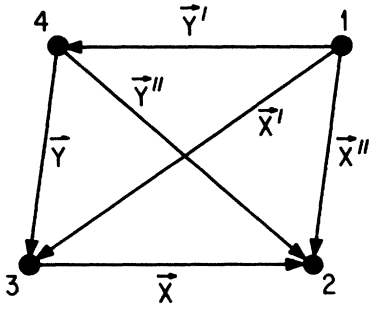

FIG. 5. Coordinate vectors of three-quark subsystems used in Eqs. (5) to define quark cluster probabilities in the $A=4$ nucleus.

V. UNIVERSALITY OF QUARK CLUSTER PROBABILITIES

We now assemble a selection of the results for $A=2$, 3, and 4 in order to examine their universality when plotted versus the dimensionless quantity $\eta=R_c/(r_m/A^{1/3})$. In

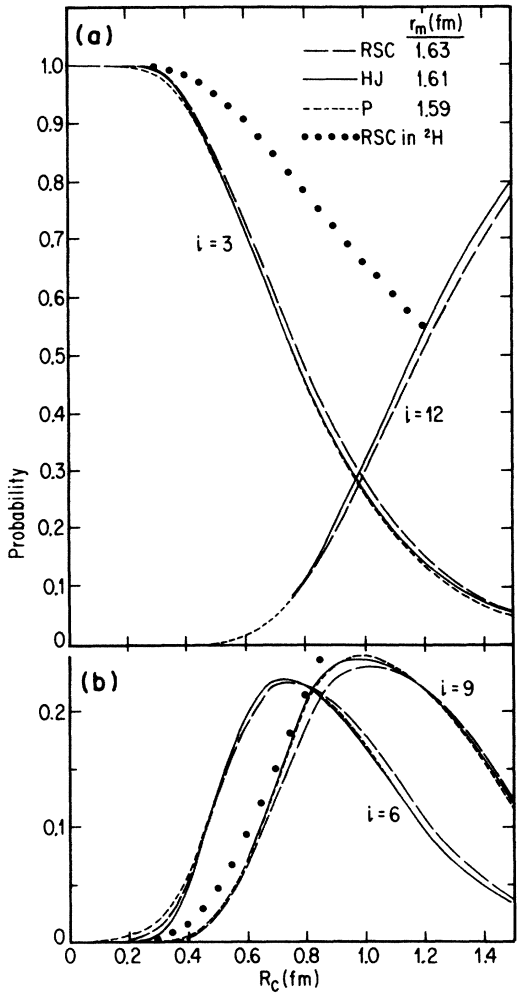

FIG. 6. i-quark cluster probabilities $\tilde{p}_i^{(4)}$ from three model wave functions of ^{4}He. Notation as in Fig. 3. The p and HJ potentials have nearly the same $\tilde{p}_i^{(12)}$ as a function of R_c. The experimental value of r_m is $\sim 1.45\pm 0.01$ fm. Also included is $\tilde{p}_i^{(2)}$ from the RSC deuteron.

Figs. 6 and 7, we displayed the deuteron results for the RSC potential along with the ^{4}He results. Dramatic differences are seen in Fig. 6 when results are plotted as a simple function of R_c. It is well known that the weakly bound deuteron has a very diffuse density compared to the tightly bound ^{4}He. Thus, when we replot vs η, we are introducing a simple scale change to approximately correct for this density difference. This appears to work very well, as the results in Fig. 7 indicate. Through the range $R_c \leq 0.8$ fm, or $\eta \leq 0.5$, the results for $\tilde{p}_3^{(2)} \approx \tilde{p}_3^{(4)}$ and $\tilde{p}_6^{(2)} \approx \tilde{p}_6^{(4)}$. In fact, the residual discrepancies in Fig. 7(b) for $\tilde{p}_6$ can be largely understood by the fact that $\tilde{p}_6^{(2)}$ is depleted by the buildup of $\tilde{p}_9^{(4)}$. Due to the good agreement between $\tilde{p}_3^{(2)}$ and $\tilde{p}_3^{(4)}$, we surmise, in fact, that

$$\tilde{p}_6^{(2)} \simeq \tilde{p}_6^{(4)} + \tilde{p}_9^{(4)} + \tilde{p}_{12}^{(4)} .$$

To further examine this issue of universality, we take the HJ potential results for $A = 2$, 3, and 4 and plot them vs R_c in Fig. 8(a). The effect of different average densities is clearly evident. However, when plotted vs η in Fig. 8(b), we again observe strong universal behavior. The exception is $\tilde{p}_6^{(2)}$, which is a special case compared to other light systems, since there is no depletion due to formation of larger clusters.

The demonstration of these universal features in our results has two major benefits for the application of the quark cluster model. First, in light nuclei, where high energy lepton data is plentiful, we can use the experimental rms radius to "correct" the quark cluster probabilities obtained from realistic wave functions whose rms radius is in error.[16,20,21] Second, we can use the results from ^{4}He

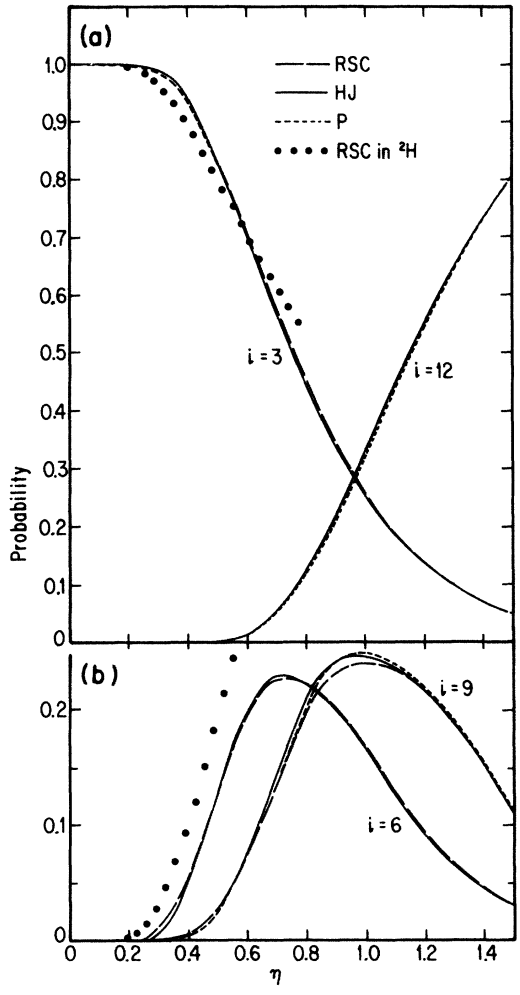

FIG. 7. The same i-quark probabilities $\tilde{p}_i^{(4)}$ in ^{4}He and $\tilde{p}_i^{(2)}$ of ^{2}H from Fig. 6 plotted as a function of $\eta = R_c/(r_m/A^{1/3})$.

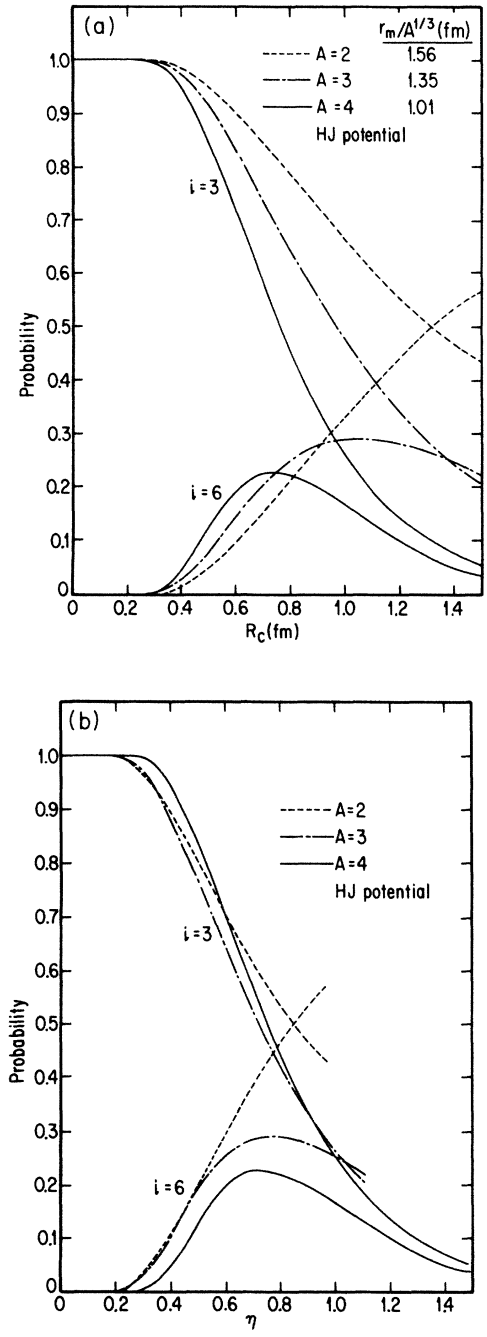

FIG. 8. i-quark cluster probabilities $\tilde{p}_3^{(A)}$ and $\tilde{p}_6^{(A)}$ in the series $A = 2$, 3, and 4 calculated with the Hamada-Johnston potential. (a) has R_c as the abscissa and (b) displays the same probabilities as a function of $\eta = R_c/(r_m/A^{1/3})$.

TABLE I. $A=2$, Reid soft core (r_m radius=1.9567 fm, expt=1.9560±0.0068 fm).

R_c	η	$\tilde{p}_3$	$\tilde{p}_6$
0.30	0.193	0.997	0.003
0.35	0.225	0.992	0.008
0.40	0.258	0.984	0.016
0.45	0.290	0.971	0.029
0.50	0.322	0.953	0.047
0.55	0.354	0.931	0.069
0.60	0.386	0.906	0.094
0.65	0.419	0.878	0.122
0.70	0.451	0.848	0.152
0.75	0.483	0.817	0.183
0.80	0.515	0.785	0.215

TABLE II. $A=3$, Malfliet-Tjon V (scalar $r_m=1.73$ fm, expt=1.70±0.02 fm).

R_c	η	$\tilde{p}_3$	$\tilde{p}_6$	$\tilde{p}_9$
0.30	0.250	0.985	0.015	0.000
0.35	0.292	0.967	0.031	0.002
0.40	0.334	0.946	0.050	0.004
0.45	0.375	0.918	0.075	0.007
0.50	0.417	0.883	0.103	0.014
0.55	0.459	0.844	0.134	0.022
0.60	0.500	0.799	0.163	0.038
0.65	0.542	0.751	0.193	0.056
0.70	0.584	0.695	0.223	0.082
0.75	0.625	0.645	0.244	0.111
0.80	0.667	0.596	0.260	0.144

along with experimental rms radii to predict the quark cluster probabilities in heavier nuclei.

With both these goals in mind, we present representative results for $A=2$, 3, and 4 using $0.3 \leq R_c \leq 0.8$ fm in Tables I–III.

Then, in Table IV, we exploit universality in η to make predictions of quark cluster probabilities in $A \geq$ nuclei. We utilize the results in Table III as a function of η and employ $R_c=0.50$ fm along with the experimental value of r_m to determine a value of η for each nucleus including $A=4$. For the $A=4$ case, this can be interpreted as a correction at $R_c=0.50$ fm, based on the fact that the Paris potential gives $r_m=1.59$ fm, while the experimental value[21] is $r_m=1.45\pm0.01$ fm.

The procedure allows us to predict $\tilde{p}_i^{(A)}$ values only up to $i=12$ quark clusters, but the rapid falloff in probabilities at this value of R_c suggests very small probabilities for clusters with $i>12$.

Note that the probabilities in ^{4}He are anomalous among the results for light nuclei and, in fact, they are rather similar to the values in ^{208}Pb.

Among the nuclei chosen for consideration, ^{197}Au provided the largest probabilities for $i>3$ and ^{9}Be the smallest. Experiments with these nuclei should provide sharp contrast in the contributions of $i>3$ quark clusters.

VI. ALTERNATIVE DEFINITIONS OF QUARK CLUSTER PROBABILITIES

Two definitions of quark cluster probabilities occur frequently in the literature, and here we present the distinctions between them. We also show explicitly how to transform between them and present those transformations explicitly in the $A=2$, 3, and 4 cases.

The first definition is the one we have employed consistently throughout our earlier efforts[1,2,6] as well as here. The quantity $\tilde{p}_i^{(A)}$ is the probability that a quark chosen at random from the nucleus A is obtained from an i-quark cluster. The second definition corresponds to the square of an amplitude in a cluster expansion of the nuclear wave function. In the second definition, one writes the total nuclear wave function as

$$|\psi(A)\rangle=\alpha\,|3q\rangle+\beta\,|6q,3q\rangle+\gamma\,|9q,3q\rangle+\delta\,|9q,6q,3q\rangle+\cdots\,, \tag{6}$$

where the first term represents only $3q$ clusters present in the nucleus, the second term represents only $6q$ and $3q$ clusters present, etc. The configurations are therefore orthogonal and assumed normalized so that $|\alpha|^2+|\beta|^2+|\gamma|^2+|\delta|^2+\cdots=1$. The full expansion in Eq. (6) can be quite complicated for the general case. Therefore let us concentrate on the light nuclei to relate these two definitions.

For the simplest case, the deuteron, the second definition implies that we write

$$|\psi(2)\rangle=A\,|3q\rangle+B\,|6q\rangle\,, \tag{7}$$

and we define $p_A^{(2)}\equiv|A|^2$, $p_B^{(2)}\equiv|B|^2$. Here the situation is straightforward, since all the quarks in the first term are in $3q$ clusters and all the quarks in the second term are in $6q$ clusters. Hence we conclude

$$\tilde{p}_3^{(2)}=p_A^{(2)}\,,\qquad \tilde{p}_6^{(2)}=p_B^{(2)}\,. \tag{8}$$

TABLE III. $A=4$, Paris ($r_m=1.59$ fm, expt=1.45±0.01 fm).

R_c	η	$\tilde{p}_3$	$\tilde{p}_6$	$\tilde{p}_9$	$\tilde{p}_{12}$
0.30	0.299	0.984	0.016	0.000	0.000
0.35	0.349	0.965	0.034	0.001	0.000
0.40	0.399	0.937	0.059	0.004	0.000
0.45	0.448	0.896	0.090	0.013	0.001
0.50	0.498	0.841	0.129	0.027	0.003
0.55	0.548	0.779	0.167	0.047	0.007
0.60	0.598	0.717	0.195	0.074	0.014
0.65	0.648	0.651	0.216	0.101	0.032
0.70	0.698	0.585	0.231	0.136	0.047
0.75	0.747	0.519	0.231	0.170	0.080
0.80	0.797	0.457	0.226	0.201	0.116

TABLE IV. Quark cluster probabilities for nuclei based upon $R_c=0.50$ fm and upon the results of the Paris potential for $A=4$. We use experimental values of charge rms radii (Refs. 21. and 22) corrected for finite proton charge contributions (we use $\langle r_p\rangle^{1/2}=0.080$ fm) to determine r_m and use this r_m to determine η. This value of η is then used to predict $\tilde{p}_i^{(A)}$ values from the Paris results for ^{4}He, given in Table III.

Nucleus	Expt. r_m (fm)	η	$\tilde{p}_3$	$\tilde{p}_6$	$\tilde{p}_9$	$\tilde{p}_{12}$
^{4}He	1.45	0.547	0.780	0.166	0.047	0.007
^{9}Be	2.38	0.437	0.905	0.083	0.011	0.001
^{12}C	2.32	0.493	0.847	0.125	0.026	0.003
^{16}O	2.59	0.486	0.854	0.120	0.024	0.003
^{20}Ne	2.91	0.466	0.876	0.104	0.018	0.002
^{24}Mg	2.97	0.486	0.854	0.120	0.024	0.003
^{27}Al	2.95	0.508	0.829	0.137	0.031	0.004
^{40}Ca	3.37	0.507	0.830	0.136	0.031	0.004
^{56}Fe	3.68	0.520	0.814	0.146	0.036	0.005
^{58}Ni	3.70	0.523	0.810	0.148	0.037	0.005
^{90}Zr	4.19	0.535	0.795	0.157	0.042	0.006
^{107}Ag	4.47	0.531	0.800	0.154	0.040	0.006
^{184}W	5.36	0.531	0.800	0.154	0.040	0.006
^{197}Au	5.24	0.555	0.770	0.171	0.051	0.008
^{208}Pb	5.44	0.545	0.783	0.165	0.046	0.007
^{238}U	5.79	0.535	0.795	0.157	0.042	0.006

The next simplest case is $A=3$, where the second definition implies we write

$$|\psi(3)\rangle = A\,|3q\rangle + B\,|6q,3q\rangle + C\,|9q\rangle \tag{9}$$

and define $p_A^{(3)} \equiv |A|^2$, etc. Now, to form $\tilde{p}_3^{(3)}$, for example, we note that both the first and the second terms contribute. A quark chosen at random from the second configuration will be in a $6q$ cluster two-thirds of the time and in a $3q$ cluster one-third of the time. Thus, it is easy to see that

$$\begin{aligned}\tilde{p}_3^{(3)} &= p_A^{(3)} + \tfrac{1}{3}p_B^{(3)}\,,\\ \tilde{p}_6^{(3)} &= \tfrac{2}{3}p_B^{(3)}\,,\\ \tilde{p}_9^{(3)} &= p_C^{(3)}\,.\end{aligned} \tag{10}$$

The sum of terms on the left gives unity, as does the sum of terms on the right. Furthermore, these equations are easily inverted to yield

$$\begin{aligned}p_A^{(3)} &= \tilde{p}_3^{(3)} - \tfrac{1}{2}\tilde{p}_6^{(3)}\,,\\ p_B^{(3)} &= \tfrac{3}{2}\tilde{p}_6^{(3)}\\ p_C^{(3)} &= \tilde{p}_9^{(3)}\,.\end{aligned} \tag{11}$$

This shows that the condition $\tilde{p}_3^{(3)} \geq (\frac{1}{2})\tilde{p}_6^{(3)}$ must hold to preserve the non-negative nature of $p_A^{(3)}$. This condition is seen to hold in the $A=3$ results presented earlier.

Continuing with $A=4$, the second definition implies that we write

$$\begin{aligned}|\psi(4)\rangle = A\,|3q\rangle + B\,|6q,3q\rangle + C\,|9q,3q\rangle\\ + D\,|6q,6q\rangle + E\,|12q\rangle\,.\end{aligned} \tag{12}$$

This time, the first three terms all contribute to $\tilde{p}_3^{(4)}$. By the procedure established in the $A=3$ example, we see that

$$\begin{aligned}\tilde{p}_3^{(4)} &= p_A^{(4)} + \tfrac{1}{2}p_B^{(4)} + \tfrac{1}{4}p_C^{(4)}\,,\\ \tilde{p}_6^{(4)} &= \tfrac{1}{2}p_B^{(4)} + p_D^{(4)}\,,\\ \tilde{p}_9^{(4)} &= \tfrac{3}{4}p_C^{(4)}\,,\\ \tilde{p}_{12}^{(4)} &= p_E^{(4)}\,.\end{aligned} \tag{13}$$

Clearly this procedure can be continued to larger nuclei with associated increase in complexity. We have presented this discussion with the hope of clearing up some confusion that has arisen due to differing definitions of quark cluster probabilities in the literature. It should facilitate comparisons of results obtained using different definitions.[12,13,23]

We have presented results for quark cluster probabilities in the $A=2$, 3, and 4 nuclei based on the assumptions of the quark cluster model. Numerical evaluations based on realistic nuclear wave functions were performed for the probability that a quark chosen at random in the nucleus is found in a color singlet cluster consisting of 3,6,9,etc., quarks. We indicated how this definition of quark cluster probability differs from others in use. A systematic comparison of cluster probabilities obtained for these light nuclei establishes an approximate scaling relationship useful for extrapolation to heavier systems. The dimensionless

parameter in which scaling was found to occur is the ratio of $A^{1/3}R_c$ to the root-mean-square radius of the baryon matter distribution obtained from the realistic wave function. Results for quark cluster probabilities in $A>4$ nuclei were presented based on this scaling relationship.

This work was supported in part by the U.S. Department of Energy under Contract No. DE-AC02-82ER40068, Division of High Energy and Nuclear Physics and the National Science Foundation Grant No. PHY-8208044.

---

*Permanent address: Sapporo Gakuin University, 11 Bunkyodai Ebetushi, 069-01, Japan.

[1]H. J. Pirner and J. P. Vary, Phys. Rev. Lett. **46**, 1376 (1981); Nucl. Phys. **A358**, 413c (1981).

[2]H. J. Pirner, in *Progress in Particle and Nuclear Physics,* edited by A. Faessler (Pergamon, Oxford, 1985), p. 361; J. P. Vary, Nucl. Phys. **A418**, 195c (1984).

[3]D. Day *et al.*, Phys. Rev. Lett. **43**, 1143 (1979).

[4]J. J. Aubert *et al.*, Phys. Lett. **123B**, 273 (1983); R. G. Arnold *et al.*, Phys. Rev. Lett. **51**, 534 (1983).

[5]C. E. Carlson and T. J. Havens, Phys. Rev. Lett. **51**, 261 (1983).

[6]J. P. Vary, S. A. Coon, and H. J. Pirner, in *Few Body Problems in Physics,* edited by B. Zeitnitz (North-Holland, Amsterdam, 1984), Vol. II, p. 683; *Proceedings of the International Conference on Nuclear Physics,* edited by R. A. Ricci and P. Blasi (Tipografia Compositori, Bologna, 1983), p. 320; *Hadronic Probes and Nuclear Interactions—1985 (Arizona State University),* Proceedings of the International Conference on Hadronic Probes and Nuclear Interactions, AIP Conf. Proc. No. **133**, edited by J. Comfort *et al.* (AIP, New York, 1985), p. 83.

[7]R. V. Reid, Ann. Phys. (N.Y.) **50**, 411 (1968).

[8]T. Hamada and I. D. Johnston, Nucl. Phys. **34**, 382 (1962).

[9]R. Tamagaki, Prog. Theor. Phys. **39**, 91 (1968).

[10]M. Lacombe *et al.*, Phys. Rev. C **21**, 861 (1980).

[11]R. A. Malfliet and J. A. Tjon, Nucl. Phys. **A127**, 161 (1969).

[12]G. Karl, G. A. Miller, and J. Rafelski, Phys. Lett. **143B**, 326 (1984).

[13]V. Koch and G. A. Miller, Phys. Rev. C **31**, 602 (1985); **32**, 1106(E) (1985); see also, Y. E. Kim, Kr. T. Kim, and R. A. Brandenburg, Phys. Lett. **160B**, 231 (1985).

[14]Y. Akaishi, M. Sakai, J. Hiura, and H. Tanaka, Prog. Theor. Phys. **51**, 143 (1974); Prog. Theor. Phys., Suppl. **56**, 6 (1974).

[15]J. L. Friar, B. F. Gibson, E. L. Tomusiak, and G. L. Payne, Phys. Rev. C **24**, 665 (1981).

[16]B. Frois, quoted in C. R. Chen, G. L. Payne, J. L. Friar, and B. F. Gibson, submitted to Phys. Rev. C.

[17]M. Sakai, I. Shimodaya, Y. Akaishi, J. Hiura, and H. Tanaka, Prog. Theor. Phys. **51**, 155 (1974); Prog. Theor. Phys., Suppl. **56**, 32 (1974).

[18]T. Katayama and M. Sakai, *Few Body Problems in Physics, Vol. II—Contributed Papers,* edited by B. Zeitnitz (North-Holland, Amsterdam, 1984) p. 435.

[19]Y. Akaishi, Nucl. Phys. **A416**, 409c (1984).

[20]Values of r_m for various potential models of ^{2}H and r_m deduced from data are found in S. Klarsfied, J. Martorell, and D. W. L. Sprung, J. Phys. **10**, 165 (1984). The "rms radius of ^{3}H" listed in Ref. 14 is, in reality, the isoscalar rms radius r_m.

[21]A precise value of the charge radius of ^{4}He is found in I. Sick, J. S. McCarthy, and R. R. Whitney, Phys. Lett. **64B**, 33 (1976).

[22]C. W. de Jager, H. de Vries, and C. de Vries, At. Data Nucl. Data Tables **14**, 479 (1974).

[23]Some early definitions of quark cluster probabilities are discussed in the reviews of Ref. 2. Others can be found in: P. Hoodbhoy and L. S. Kisslinger, Phys. Lett. **146B**, 163 (1984); M. Namiki *et al.*, Phys. Rev. C **25**, 2157 (1982); M. A. Maize and Y. E. Kim, *ibid.* **25**, 1923 (1985); V. V. Buro *et al.*, Z. Phys. A **306**, 149 (1982); A. P. Kobyshikin and L. Vizireva, J. Phys. G **8**, 893 (1982); J. Dias de Deus *et al.*, Z. Phys. C **26**, 190 (1984); Phys. Rev. D **30**, 697 (1984); B. C. Clark *et al.*, *ibid.* **31**, 617 (1985); M. Chemtob and R. Peschanski, J. Phys. G **10**, 599 (1984); R. Jaffe *et al.*, Phys. Lett. **134B**, 449 (1984); H. Faissner, B. R. Kim, and H. Reithler, Phys. Rev. Lett. **54**, 1902 (1984).